如需购买此标准物质，请联系我们：15812817678 陈经理（微信同号）

National Institute of Standards & Technology

Certificate of Analysis

Standard Reference Material® 1879b

Respirable Cristobalite
(Quantitative X-Ray Powder Diffraction Standard)

This Standard Reference Material (SRM) is intended for use in preparation of calibration standards for quantitative analyses of cristobalite by X-ray powder diffraction in accordance to National Institute for Occupational Safety and Health (NIOSH) Analytical Method 7500 [1] or equivalent. A unit of SRM 1879b consists of approximately 5 g of powder bottled in an argon atmosphere.

Material Description: The SRM material was prepared from high purity fused quartz powder, which was annealed at 1600 °C for 2 h. This operation was done in a furnace that allowed for insertion of the SRM material at the operating temperature and under a controlled atmosphere. The resulting high porosity sintered form was crushed and jet milled to a median particle size of 3.5 μm. The powder was treated with hydrofluoric and hydrochloric acids to reduce phase and elemental contamination. An analysis of the quantitative results from Rietveld analyses of X-ray powder diffraction data indicated that the SRM material was homogeneous with respect to diffraction properties.

Certified Values: A NIST certified value is a value for which NIST has the highest confidence in its accuracy in that all known or suspected sources of bias have been investigated or taken into account. The measurands are the certified values for the crystalline phase purity of the material (cristobalite) and the lattice parameters are provided in Table 1. Metrological traceability is to the SI units for the derived unit of mass fraction (expressed as milligrams per kilogram), and for length (expressed as nanometers); for crystalline phase purity and lattice parameters, respectively. The certified values and uncertainties were calculated according to the method described in the ISO/JCGM Guide [2].

Information Values: An information value is considered to be a value that will be of interest and use to the SRM user, but insufficient information is available to adequately assess the uncertainty associated with the value, or it is a value derived from a limited number of analyses. Information values cannot be used to establish metrological traceability. The information values for the particle size distribution, as determined by laser scattering, are given in Figure 1.

Expiration of Certification: The certification of **SRM 1879b** is valid indefinitely, within the measurement uncertainty specified, provided the SRM is handled and stored in accordance with instructions given in this certificate (see “Instructions for Storage and Use”). Periodic recertification of this SRM is not required. The certification is nullified if the SRM is damaged, contaminated, or otherwise modified.

Maintenance of SRM Certification: NIST will monitor this SRM over the period of its certification. If substantive changes occur that affect the certification, NIST will notify the purchaser. Registration (see attached sheet or register online) will facilitate notification.

Overall coordination and technical direction of the certification were performed by J.P. Cline of the NIST Materials Measurement Science Division.

Material preparation, measurements, and data analysis leading to the certification of this SRM were provided by J.P. Cline, D. Black, M.H. Mendenhall, and A. Henins of the NIST Materials Measurement Science Division.

P.S. Whitfield of Oak Ridge National Laboratory contributed to the analysis of the neutron data.

John A. Small, Chief
Materials Measurement Science Division

Gaithersburg, MD 20899
Certificate Issue Date: 16 November 2017

Steven J. Choquette, Director
Office of Reference Materials

A portion of this research used resources at the Spallation Neutron Source, a DOE Office of Science User Facility operated by the Oak Ridge National Laboratory.

Collection of the laser scattering particle size data for informational value was performed by M. Peltz of the NIST Materials and Structural Systems Division.

Statistical analysis was performed by J.J. Filliben of the NIST Statistical Engineering Division.

Support aspects involved in the issuance of this SRM were coordinated through the NIST Office of Reference Materials.

INSTRUCTIONS FOR STORAGE AND USE

Storage: SRM 1879b was bottled in an argon atmosphere to protect against humidity. NIST has not performed any studies concerning the possible degradation of the diffraction properties of cristobalite, SRM 1879b, as a function of a long-term exposure to humidity. Nor are we aware of any published work concerning this issue. However, SRM 1879b is a high surface area powder; some reactivity to moisture, if only physisorption, is possible. It is recommended that the unused portion of this powder be stored in the original bottle, tightly capped in a dry atmosphere.

SOURCE, PREPARATION, AND ANALYSIS[(1)]

Materials: The feedstock for SRM 1879b was prepared with a high-temperature anneal of vitreous silica. The starting material was of a purity greater than 99.995 % (by weight), with less than 25 parts per million alkali. It was annealed at 1600 °C in an induction furnace that allowed for insertion of the SRM material at the operating temperature and under a controlled atmosphere. The material was annealed for 2 h after the furnace temperature had re-equilibrated to 1600 °C at which point the furnace was powered down and allowed to cool. This annealing operation was performed by Pyromatics Corp. (Willoughby, OH). The resulting high porosity sintered form was processed in a jaw crusher and jet milled to a median particle size of 3.5 μm. The jet milling was performed by Hosokawa Micron Powder Systems (Summit, NJ). The disordered, amorphous surface region of the powder was preferentially dissolved with a wash in hydrofluoric acid. Additional contaminants were removed with second wash in hydrochloric acid. The powder was then rinsed several times in distilled water and ignited at 500 °C. These treatments were performed by MV Laboratories, Inc. (Frenchtown, NJ).

Phase Purity: A long-count-time X-ray powder diffraction pattern of SRM 1879b will offer data consistent with a high-purity cristobalite powder. However, the surface region of any crystalline material will not diffract as the bulk due to relaxation of the crystal structure and inclusion of surface reaction products. While this disordered, amorphous surface layer may only be on the order of a few crystallographic units in thickness, in a finely divided solid it can easily account for several percent of the total mass. Phase purity as discussed herein is a microstructural characteristic innate to a finely divided crystalline solid and influenced by the production history of the cristobalite powder used as the feedstock.

Certification Method: The certified measurement values of SRM 1879b include the crystalline phase purity and the lattice parameters. Ancillary data include the particle size distribution determined via laser scattering and microstructural information determined from the X-ray experiments. The data that led to the certification of phase purity consisted of neutron time-of-flight (TOF) and constant wavelength (CW) powder diffraction data. TOF data were collected on the POWGEN beamline at the Spallation Neutron Source [3], ORNL. The CW neutron data were collected on the BT1 High Resolution Powder Diffractometer located at the NIST Center for Neutron Research (NCNR) [4]. SRM 676a Alumina Powder for Quantitative Analysis by X-Ray Diffraction, which was certified with respect to amorphous content [5,6], was used as the internal standard in all diffraction experiments. The phase purity of SRM 1879b was certified through an analysis of the discrepancy between the mass fractions of cristobalite and alumina determined from Quantitative Rietveld Analysis (QRA) [7], relative those of the weighing operation. QRA yields only the mass fractions of the crystalline materials; whereas the weighing operation includes both the crystalline and amorphous components. Neutron data are considered to be essentially free of a systematic bias in phase quantification that is often observed in analyses of laboratory X-ray powder diffraction data.

Laboratory XRD data were collected on a NIST-built diffractometer set up in two configurations. A full discussion of this machine, its alignment and calibration can be found in reference 8. The first configuration consisted of a

[(1)] Certain commercial instruments, materials, or processes are identified in this certificate to adequately specify the experimental procedure. Such identification does not imply recommendation or endorsement by the National Institute of Standards and Technology, nor does it imply that the instruments, materials, or processes identified are necessarily the best available for the purpose.

conventional Cu Kα source and linear Si-strip position sensitive detector (PSD). The second utilized a Johansson Ge [111] incident beam monochromator (IBM) and PSD. Data analyses were performed with the fundamental parameters approach (FPA) [9] for line profile modeling in conjunction with the Pawley [10] and Rietveld methods for analysis of lattice and structural parameters. The homogeneity of SRM 1879b was verified with an analysis of the mass fractions of quartz versus alumina and the lattice parameters of in specimens that consisted of 50-50 mixtures of SRMs 1878b and 676a. The linkage of the certified lattice parameter values to the fundamental unit for length, as defined by the International System of Units (SI) [11], was established with use of the emission spectrum of Cu Kα radiation as the basis for constructing the diffraction profiles. With the use of the FPA, diffraction profiles are modeled as a convolution of functions that describe the wavelength spectrum, the contributions from the diffraction geometry, and the sample contributions resulting from microstructural features. Analysis of data from a divergent-beam instrument requires knowledge of both the diffraction angle and the effective source sample detector distance. Two additional models are therefore included in the FPA analyses to account for the factors that affect the sample height and attenuation. Certification data were analyzed in the context of both Type A uncertainties, assigned by statistical analysis, and Type B uncertainties, based on knowledge of the nature of errors in the measurements, to result in the establishment of robust uncertainties for the certified values.

Certification Procedure: Ten bottles of SRMs 1879b and 676a (internal standard) were removed from their respective populations in accordance to a stratified random protocol. All samples consisted of 50:50 mixes of SRMs 1879b and 676a. Five samples were prepared for neutron diffraction analysis with each sample consisting of four grams of material, 1 g from each of two randomly selected bottles of SRMs 1879b and 676a. For X-ray powder diffraction analyses, two specimens were prepared from each bottle of SRM 1879b for a total of 20 samples consisting of 50:50 mixtures; the mass of these specimens was 1 g. Both the order in which the specimens were prepared and the bottle of SRM 676a used were randomized. All specimens were homogenized with a kneading operation with a mortar and pestle. Five additional, phase pure specimens were mounted for determination of certified lattice parameters.

With the collection of TOF neutron diffraction data at POWGEN, approximately 3 g of sample were loaded in 8 mm diameter vanadium cans for data collection using a 0.1 nm band centered on a wavelength of 0.1333 nm at 300 °K. This resulted in diffraction patterns with d-spacing spans from 0.04 nm to 0.53 nm. The data were collected for 3 beam hours at an accelerator power of 850 kW. With the CW neutron data, samples were contained cylindrical vanadium cans of 12.4 mm in diameter by 50 mm high during the measurement. Data were collected for approximately 14 h at a wavelength of 0.11969 nm by the [733] reflection from a Ge monochromator with a collimation of 60', 30', and 7', before the monochromator, sample and detectors, respectively, with a 120° take off angle. This allowed for a d-spacing range in the data from 0.06 nm to 0.56 nm. The run order was randomized on an informal basis.

The neutron diffraction data were analyzed with a QRA in two global refinements of the 5 data sets; one refinement for each diffraction method. The analyses of the TOF data was done utilizing the TOPAS [12] while that of the CW was done using General Structure Analysis System (GSAS) [13]. The crystal structure for low cristobalite as reported by O'Keefe and Hyde [14] was used in these analyses. The refined parameters common to both analyses included: scale factors, lattice parameters of SRM 1879b, and structural parameters. With respect the analysis of TOF data, calibration runs on POWGEN using SRM 660b, Line Position and Line Shape Standard for Powder Diffraction [15,16], were used to determine values for DIFC, DIFA and zero, and starting values for terms of the GSAS-style TOF profile function "type -3" [17]; i.e. back-to-back exponentials (α_0, α_1, β_0, β_1) convoluted with a pseudo-Voigt with a d-spacing and $(\text{d-spacing})^2$ dependence. With the analysis of the SRM 1879b / 676a mixtures, terms pertaining to an additional pseudo-Voigt size broadening also with a d-spacing and $(\text{d-spacing})^2$ dependence were refined. They were constrained across histograms and phases. The lattice parameters of the alumina of SRM 676a were fixed at certified values and the diffractometer constant DIFA was refined. The back-to-back exponential terms α_0, α_1, β_0 and β_1 were also refined, with only small changes from the SRM 660b values; these were constrained with respect to the histograms. The TOF refinement included 4 terms of a shifted Chebyshev background function. To fit a contribution to the background from diffuse scattering evident at high Q, a second derivative Debye term with a thermal motion correction was used. The starting value of the atomic distance term r was the cristobalite Si-O bond distance of 0.164 nm. The terms of the function were constrained across the histograms while a background scale factor was refined independently for each histogram.

The CW neutron data were analyzed using the GSAS profile function "type 3" [18]. Refined terms included GU, GV, GW, LX, LY and SL; all were constrained by phase and histogram. The Finger [19] model was used to account for profile asymmetry; however, the S/L and H/L terms are highly correlated, only one term, SL, was refined while the other was fixed at a value nominally identical to the first. Also, given that the lattice parameters of the SRM 676a phase were fixed, the wavelength and zero values were refined. The CW refinement included 7 terms of a shifted Chebyshev background function.

The crystalline phase content was determined from the mass fractions determined from the diffraction experiment relative to those of the weighing operation, with the latter ratio being corrected for the known crystalline phase purity of SRM 676a. Considering the results from the two data collections methods independently, the mean for the results from the TOF experiments was 94.37 % crystalline cristobalite, while the mean for the CW experiments is 93.58 %. The difference between these two means being statistically significant; they were combined with a "Mean of Means" method to yield the certified value and $k = 2$ expanded uncertainty for the certified crystalline phase purity. The certified crystalline phase purity is shown in Table 1.

With the collection of X-ray powder diffraction data using the conventional X-ray source, the 2.2 kW copper tube of long fine focus geometry was operated at a power of 1.8 kW. With the IBM, the 1.5 kW copper tube of fine focus geometry was operated at a power of 1.2 kW. The variable divergence incident slit was set to 0.9°. The scan time was approximately 2.5 hours. A 1.5° Soller slit was located in front of the PSD window to limit axial divergence, no Soller slits were used in the incident beam either configuration. The PSD was scanned using a variable window length and a combination of coarse and fine steps in θ/2θ was used that allowed for data to be collected at high resolution in a timely manner [20]. With the conventional X-ray source, a nickel filter was included in the PSD entrance window. Samples were spun at 0.5 Hz during data collection. The machine was equipped with an automated anti-scatter slit that blocked air scatter from the incident beam from entering the PSD, where it would otherwise contribute to the low angle background level. It is located above the specimen, the initial installation limited the high angle range to 140 °2θ; later, it was modified to permit the full range of data collection, from 18 °2θ to 155 °2θ. The machine was located within a temperature-controlled laboratory space where the nominal short-range control of temperature was ± 0.1 K. The temperature was monitored using two 10 kΩ thermistors with a Hart/Fluke BlackStack system that was calibrated at the NIST temperature calibration facility [21] to ± 0.002 °C. The source equilibrated at operating conditions for at least an hour prior to recording any certification data. The performance of the machine was qualified with the use of SRMs 660b and 676a using procedures discussed by Cline *et al*. [8].

The certification data were analyzed using the FPA method with Rietveld and Pawley analyses as implemented in TOPAS. Mendenhall *et al*. [22] verified that TOPAS operated in accordance with published models for the FPA. The analysis used energies of the Cu $K\alpha_1$ emission spectrum as characterized by G. Hölzer, *et al*. [23]. The refined parameters included the scale factors, Chebyshev polynomial terms for modeling of the background, the lattice parameters, specimen displacement and attenuation terms, structural parameters (with the Rietveld analyses), terms for Lorentzian size and, in the case of the cristobalite, strain broadening. A discussion of the incident spectrum from the IBM and the approach used in its modeling, as well as the characterization of the instrument profile function (IPF) via the FPA are discussed in Cline *et al*. [8]. The procedure used high-count-time data collected from SRM 660b using a relatively small divergence slit angle of 0.5°. The incident spectrum was then modeled with a refinement of the breadths and intensities of three Gaussian profiles at the $K\alpha_{11}$ location, as defined by Hölzer, and a fourth one located at the $K\alpha_{12}$ location. Additional refined parameters included the Soller slit angles with the "full" axial divergence model [24]. This analysis provided parameters describing the incident beam spectrum and Soller slit angles characterizing the IPF of the instrument utilizing the IBM. Additional FPA analyses of SRM 660b, using data collected as per SRM 1879b with both conventional and IBM configurations, was performed. This provided a final check on IPF parameters, such as the equatorial angle the incident slit and the "receiving slit size"; with the use of the PSD this is actually the equatorial width of the silicon strips. With analyses of SRM 1879b, these IPF specific values were held fixed at these predetermined values. The refined lattice parameters from the five phase pure specimens, analyzed with the Pawley method were adjusted using the coefficient of thermal expansion values found in Peacor *et al*. [25] to values in correspondence with 22.5 °C.

The measurand is the certified value for lattice parameters obtained with TOPAS via the Pawley method is shown in Table 1. The statistical, Type A, evaluation of the lattice parameters resulted in estimates of the lattice parameters of a = 0.497 082 68 nm and c = 0.691 955 76 nm with $k = 2$ expanded uncertainties of 0.000 005 16 nm and 0.000 005 91 nm for a and c, respectively. However, the components of uncertainty that were evaluated by Type B methods must also be taken into account, and these are roughly one order of magnitude larger than those that were evaluated using statistical methods. Data were considered primarily in the context of the uniformity in lattice parameter as a function of 2θ angle [26]; this, in turn, would reflect the functionality of the FPA model. This approach was applied to data from SRM 660b used to calibrate the machine, and both SRMs 676a and 1879b that were contained in the samples. These considerations lead to an assignment of a Type A + B uncertainty of 0.000 030 0 nm to the a and c lattice parameters.

Information Values: The FPA experiments included an analysis of crystallite size using the Scardi and Leoni formalism [27] for a log-normal size distribution of spherical crystallites. Owing to the lack of said broadening observed with SRM 1879b on laboratory equipment, these refinements yielded non-physical results for crystallite size. While SRM 1879b does display a slight amount of broadening varying as 1/cos θ, it is insufficient for a valid determination of crystallite size. The FWHM term varying as tan θ, interpreted as microstrain, refined to ε_0 value of 0.00022, where $(\varepsilon_0)^2$ is the mean squared strain. The refined structural parameters obtained from the Rietveld analyses

of SRM 1879b, from both the X-ray and neutron data, did not differ substantially from those reported by O'Keefe and Hyde [14]. The information values for the particle size distribution, as determined by laser scattering, are given in Figure 1.

Table 1. Certified Values for SRM 1879b

	Mass Fraction
Crystalline phase purity (low cristobalite)	93.98 % ± 0.79 %

	Lattice Parameter (nm)
a	0.497 083 ± 0.000 030
c	0.691 956 ± 0.000 030

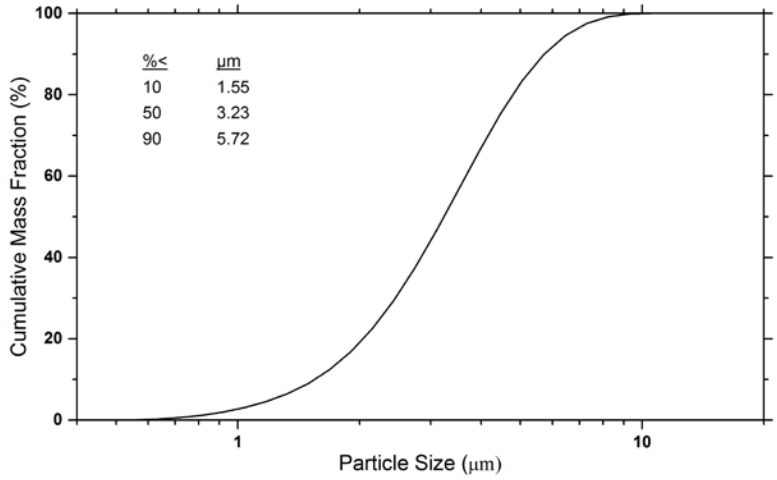

Figure 1. Typical Particle Size Distribution by Laser Scattering

REFERENCES

[1] *NIOSH Manual of Analytical Methods (NMAM®)*, 4th ed., 3rd supplement; DHHS (NIOSH) Publication No. 2003-154; Schlecht, P.C.; O'Connor, P.F., Eds. (2003).

[2] JCGM 100:2008; *Guide to the Expression of Uncertainty in Measurement*; (GUM 1995 with Minor Corrections), Joint Committee for Guides in Metrology (JCGM) (2008); available at http://www.bipm.org/utils/common/documents/jcgm/JCGM_100_2008_E.pdf (accessed Nov 2017); see also Taylor, B.N.; Kuyatt, C.E.; *Guidelines for Evaluating and Expressing the Uncertainty of NIST Measurement Results*; NIST Technical Note 1297; U.S. Government Printing Office: Washington, DC (1994); available at http://physics.nist.gov/Pubs/contents.html (accessed Nov 2017).

[3] Huq, A.; Hodges, J.P.; Gourdon, O.; Heroux, L.; *Powgen: A third-generation high-resolution high-throughput powder diffraction instrument at the Spallation Neutron Source*; Z. Kristallogr., Proc. 1, pp. 127–135 (2011). DOI 10.1524/zkpr.2011.0019.

[4] Website for High Resolution Powder Diffractometer – BT1 available at https://www.ncnr.nist.gov/instruments/bt1/ (accessed Nov 2017).

[5] SRM 676a; *Alumina Powder for Quantitative Analysis by X-ray Diffraction*; National Institute of Standards and Technology; U.S. Department of Commerce: Gaithersburg, MD (23 April 2012).

[6] Cline, J.P.; Von Dreele, R.B.; Winburn, R.; Stephens, P.W.; Filliben, J.J.; *Addressing the Amorphous Content Issue in Quantitative Phase Analysis: The Certification of NIST SRM 676a*; Acta Crystallographica Section A, Vol. A67, pp. 357–367 (2011).

[7] Rietveld, H.M.; *Line Profiles of Neutron Powder Diffraction Peaks for Structure Refinement*; Acta Crystallogr., Vol. 22, pp. 151–152 (1967); see also Rietveld, H.M.; *A Profile Refinement Method for Nuclear and Magnetic Structures*; J. Appl. Crystallogr., Vol. 2, pp. 65–71 (1969).

[8] Cline, J.P.; Mendenhall, M.H.; Black, D.; Windover, D.; Henins, A.; *The Optics and Alignment of the Divergent Beam Laboratory X-ray Powder Diffractometer and its Calibration Using NIST Standard Reference Materials*; J. Res. Natl. Inst. Stand. Technol., Vol. 120, pp. 173–222 (2015).
[9] Cheary, R.W.; Coelho, A.A.; *A Fundamental Parameters Approach to X-Ray Line-Profile Fitting*; J. Appl. Crystallogr., Vol 25, pp. 109–121 (1992).
[10] Pawley, G.S.; *EDINP, the Edinburgh Powder Profile Refinement Program*; J. Appl. Cryst., Vol. 13(6), pp. 630–633 (1980).
[11] BIPM; *International System of Units (SI)*, Bureau International des Poids et Mesures; 8th ed., Sèvres, France (2006); available at http://www.bipm.org/utils/common/pdf/si_brochure_8_en.pdf (accessed Nov 2017)
[12] Bruker AXS. Topas v5, a component of DIFFRAC.SUITE (2014); available at https://www.bruker.com/products/x-ray-diffraction-and-elemental-analysis/x-ray-diffraction/xrd-software/overview/topas.html (accessed Nov 2017).
[13] Larson, A.C.; Von Dreele, R.B.; *General Structure Analysis System (GSAS)*; Report LAUR 86-748; Los Alamos National Laboratory: Los Alamos, NM (2003).
[14] O'Keefe, M., Hyde, B.G., *Cristobalites and Topologically-Related Structures*, Acta Cryst., B32, 2923-2936 (1976).
[15] SRM 660b; *Line Position and Line Shape Standard for Powder Diffraction*; National Institute of Standards and Technology; U.S. Department of Commerce: Gaithersburg, MD (29 April 2010).
[16] Black, D.; Windover, D.; Henins, A.; Filliben, J.J.; Cline, J.P.; *Certification of Standard Reference Material 660B*; Powder Diffr., Vol. 26 (2), pp. 155–158 (2011).
[17] Von Dreele, R.B.; Jorgensen, J.D.; Windsor, C.G.; *Rietveld Refinement with Spallation Neutron Powder Diffraction Data*; J. Appl. Crystallogr., Vol. 15, pp. 581−589 (1982).
[18] Thompson, P.; Cox, D.E.; Hastings, J.B.; *Rietveld Refinement of Debye-Scherrer Synchrotron X-ray Data from Al_2O_3*; J. Appl. Crystallogr., Vol. 20, pp. 79–83 (1987).
[19] Finger, L.W.; Cox, D.E.; Jephcoat, A.P.; *A Correction for Powder Diffraction Peak Asymmetry Due to Axial Divergence*; J. Appl. Crystallogr., Vol. 27, pp. 892–900 (1994).
[20] Mendenhall, M.H.; Cline, J.P.; *Efficient Collection of X-ray Powder Diffraction Data with a Solid State Position Sensitive Detector*; J. Appl. Crystallogr., submitted.
[21] Vaughn, C.D. and Strouse, G.F.; *The NIST Industrial Thermometer Calibration Laboratory*. In 8th Int'l Symp. Temperature and Thermal Measurements in Industry and Science, Berlin, June 2001. available at http://ws680.nist.gov/publication/get_pdf.cfm?pub_id=830734 (accessed Nov 2017).
[22] Mendenhall, M. H.; Mullen, K.; Cline, J. P.; *An implementation of the Fundamental Parameters Approach for Analysis of X-ray Powder Diffraction Line Profiles*; J. Res. Natl. Inst. Stand. Technol., Vol. 120, pp. 223–251 (2015).
[23] Hölzer, G.; Fritsch, M.; Deutsch, M.; Härtwig, J.; Förster, E.; *$K\alpha_{1,2}$ and $K\beta_{1,3}$ X-Ray Emission Lines of the 3d Transition Metals*; Phys. Rev. A, Vol 56 (6), pp. 4554–4568 (1997).
[24] Cheary, R.W.; Coelho, A.A.; *Axial Divergence in a Conventional X-Ray Powder Diffractometer I. Theoretical Foundations*; J. Appl. Crystallogr., Vol. 31, pp. 851–861 (1998); see also Cheary, R.W.; Coelho, A.A.; *Axial Divergence in a Conventional X-Ray Powder Diffractometer II, Implementation and Comparison with Experiment*; J. Appl. Crystallogr., Vol. 31, pp. 862–868 (1998).
[25] Peacor, D.R.; *High-temperature Single-crystal study of the Cristobalite Inversion*; Zeitschrift fur Kristallographie, Bd. Vol. 138, S. pp. 274–298 (1973).
[26] Cline, J.P, Black, D., Gil, D., Henins, A. and D., Windover; *The Application of the Fundamental Parameters Approach as Implemented in TOPAS to Divergent Beam Powder Diffraction Data*; Materials Science Forum Vol. 651 pp. 201–219 (2010).
[27] Scardi, P.; Leoni, M.; *Diffraction Line Profiles from Polydisperse Crystalline Systems*; Acta Cryst. A, Vol. 57(5), pp. 604–613 (2001).

Users of this SRM should ensure that the Certificate of Analysis in their possession is current. This can be accomplished by contacting the SRM Program: telephone (301) 975-2200; fax (301) 948-3730; e-mail srminfo@nist.gov; or via the Internet at http://www.nist.gov/srm.